Polytypism and the vibrational properties of PbI_2

W. M. Sears,* M. L. Klein, and J. A. Morrison
Departments of Physics and Chemistry and Institute for Materials Research, McMaster University, Hamilton, Ontario, Canada
(Received 30 August 1978)

The vibrational properties of six different polytypes of PbI_2 crystals have been studied experimentally by means of Raman spectroscopy and x-ray diffraction. The crystals were prepared either by gel growth or by thermal annealing. The Raman spectra are used to determine features of the phonon dispersion curves, in the crystallographic c direction, which are common to all of the polytypes. The results are correlated with existing information obtained from measurements of Brillouin spectra and inelastic scattering of neutrons and then analyzed within the framework of a six-parameter force-constant model. Thermodynamic data, including new measurements of lattice parameters in the range $100 < T < 295$ K, are used to discuss anharmonic and two-dimensional contributions to the vibrational properties.

I. INTRODUCTION

In the solid state, a number of substances form layered structures in which bonding between layers is much weaker than within a layer. Lead iodide is an example although a less extreme one than, say, graphite or MoS_2. Because of the relative weakness of the interlayer interaction, layered crystals can be thought of in terms of planes being stacked in the c direction. There are, in general, three possible positions for each layer (as in the hcp and fcc structures for the packing of spheres). Since there is little restriction on the order of packing, unit cells of almost any repeat distance can be formed in the c direction. A well-known example is SiC which has been widely studied.[1] The number of space groups available to layered structures, in which the individual layers have hexagonal or trigonal symmetry, is limited [$P3m1$, $P\bar{3}m1$, $P\bar{6}m2$, $P6_3/mc$, $P6_3/mmc$, $R\bar{3}m$, and $F\bar{4}3m$ (see p. 159 of Ref. 1)] but the stacking order is almost unlimited. A separate type of notation is thus desirable to describe the situation; the Ramsdell notation[2] is commonly used. In PbI_2, a layer consists of a plane of lead atoms sandwiched between two planes of iodine atoms. The notation refers to the sequence of iodine atoms in PbI_2 and so a $6H$ polytype contains three complete layers. The letter refers to the Bravais lattice that results from the stacking arrangement: cubic (C), hexagonal or trigonal (H), or rhombohedral (R). In PbI_2, the cubic arrangement is not observed. PbI_2 is known to form many different polytypes but the common techniques of preparation, such as gel growth[3] or thermal annealing,[4] tend to yield a distribution of polytypes.[5] It is thus important that the structure of each crystal studied should be identified by x-ray diffraction.

The higher polytypes are of particular value in allowing Raman and infrared data to be used to obtain elements of the vibrational structure of layered crystals that are not ordinarily accessible to study by optical methods. Only the $q = 0$ portion of the dispersion curve is usually available. In polytypic substances, however, the various polytypes can be considered to share the same dispersion curves. The effect of the larger cell is then to fold back the dispersion curves in the c direction, thus making more modes accessible to the Raman and infrared techniques (at $q = 0$). This method has been used extensively in the study of the vibrational structure of SiC.[6-9]

Much of the prior work on PbI_2 has been concerned with its band structure, semiconducting properties, and exciton spectrum[10-16] and less with the vibrational properties. Raman spectra are available for the $2H$ and $4H$ polytypes, and some infrared data for $2H$.[17-21] Inelastic neutron scattering experiments have been performed on a large crystal (probable $2H$) at room temperature[22] and the results used to delineate portions of dispersion curves in particular crystallographic directions. Information about velocities of sound at room temperature have been obtained from measurements of the Brillouin spectrum.[23]

The detailed lattice dynamics of layer crystals such as ferrous chloride[24] has been studied using a shell model in which ionicity and polarization effects were included. Recently, similar calculations have been reported[25] for PbI_2 where it was found necessary to introduce a long-range interaction due to static dipoles in order to achieve reasonable agreement with observed Raman and infrared frequencies. This long-range anisotropic force cannot be caused by polarization because PbI_2 is nearly isotropic. Such dipoles could be thought of as a consequence of covalent bonding and might be treated via bond charge models.[26] Pasternak (private communication) is currently extending his shell-model calculations on ferrous

halides to include PbI_2. Recently, the $q=0$ modes of the $2H$ structure of PbI_2 have been discussed[27] on the basis of a simple nearest-neighbor, atom-atom, force-constant model. In its present form, the model is not adequate to correlate data for the higher polytypes.

The experiments to be described in this paper provide the following new information: Raman spectra of polytypes $2H$, $4H$, $6H$, $8H$, $12H$, and $12R$ at temperatures $T=50$ K and 400 K and thermal expansion for $T>100$ K. In place of microscopic models referred to above, a relatively simple linear-chain force-constant model[28] is used to correlate all of the available experimental information. The detailed interpretation of the model parameters may be somewhat uncertain, but the simplicity of the model makes it attractive to use. We will see that the two-dimensional character of the vibrational spectrum turns out to be relatively small despite the fact that PbI_2 forms structures that are clearly strongly layerlike.

II. EXPERIMENTAL

A. Preparation of crystal specimens

Some polytypes were prepared by following the techniques of gel growth described by Henisch *et al.*[3,29,30] A solution of KI was placed on top of a silica gel containing lead acetate in solution, the entire system being contained in a stoppered test tube hung in a water thermostat. Hexagonal platelets of PbI_2 were allowed to grow in the gel over a period of a few weeks. In repetetive experiments, variations were made in some of the parameters: the density and pH of the gel; concentrations of lead acetate and KI solutions; temperature. The yield of higher polytypes was smaller than that reported by Hanoka *et al.*[3] but similar to that found by others.[5,31,32] Of 89 crystals that were examined, 7 turned out to be other than pure $2H$.

A more productive method of obtaining certain polytypes turned out to be to heat $2H$ crystals that had been prepared by gel growth. The crystals were heated in an evacuated ($P<1\times10^{-4}$ Torr) glass tube to temperatures between 130 and 300 °C for periods of 1–44 h. Only $4H$, $12R$, and mixtures of the two were formed by this method, but the yields were 100% if $T>170$ °C. There has been a suggestion[32] that these polytypes, especially $12R$, are metastable and that they tend to revert to $2H$ at room temperature. We did not observe such reversion in a period of two years.

A Buerger precession camera and Mo x radiation were used in the identification of the various polytypes in lead iodide. The hexagonal platelets were easily aligned visually so as to give an x-ray photograph of the O, K, L reciprocal plane. Since all polytypes are built up from the same $2H$ layer, the photographs of the O, K, L plane superimpose over the $2H$ reflections. This makes the identification of various polytypes reasonably straightforward. It should be noted that, in the hexagonal PbI_2 structure, the polytypes have characteristic extinctions:

$$H+K=3n \quad (n=0,\ 1,\ 2,\ldots)$$

and

$$L\neq n'n/2$$

(n' is the order of polytype, e.g., $n'=4$ for $4H$). This means that it is only necessary to count the reflections which appear between the $2H$ reflections. The directions 0, 1, L; 0, 2, L; 0, $\bar{1}$, L, and 0, $\bar{2}$, L are the best to use.

For the rhombohedral polytypes, $-H+K+L\neq3n$. For the O, K, L plane (see Fig. 1), $K+L\neq3n$. The extinction can easily be identified by comparing adjacent lines (e.g., 0, 1, L and 0, 2, L). It can occur in an obverse or a reverse direction depending on crystal orientation. In fact, both obverse and reverse orientations can exist in the same crystal. Therefore, some care must be taken in separating combinations of, say, $12R$ obverse, $12R$ reverse, and $4H$, etc. The combination of $12R$ (obverse)+$12R$ (reverse)+$4H$ can appear to be the same as $12H$ in an x-ray photograph but their Raman spectra are easily distinguished.

The majority of the polytypes used in the experiments were actually composites of polytypes:

FIG. 1. X-ray photograph of polytype $12R$(reverse) of PbI_2 in the O, K, L reciprocal plane.

TABLE I. Summary of polytypes of PbI_2 which were prepared and studied.

Polytype	Space group	Vibrational modes at $q=0$
$2H$	$P\bar{3}m1$ (D_{3d}^3)	$A_{1g}+E_g+2A_{2u}+2E_u$
$4H$	$P6_3mc$ (C_{6v}^4)	$3A_1+3B_1+3E_1+3E_2$
$6H$	$P3m1$ (C_{3v}^1)	$9A_1+9E$
$8H$	$P3m1$ (C_{3v}^1)?	$12A_1+12E$
$12H$	$P3m1$ (C_{3v}^1)?	$18A_1+18E$
$12R$	$R\bar{3}m$ (D_{3d}^5)	$2A_{1g}+2E_g+4A_{2u}+4E_u$

$6H$ with $2H$, $8H$ with $4H$, etc. However, the different segments could be identified spatially in the crystals and their Raman spectra resolved unambiguously. The polytypes studied and their space groups and the designations of their vibrational modes are listed in Table I.

B. Raman spectra

A Coderg PHO laser Raman spectrometer was used for the experiments on the PbI_2 crystals. It has double Ebert Fastie gratings that cover the wavelength range 4000–9000 Å. The accuracy and reproducibility are stated to be ± 1 cm^{-1}, and this is confirmed by a comparison of results from the present experiments with some published Raman spectra for PbI_2 (see Sec. III A). The output from a photomultiplier and dc amplifier was fed into a recorder which was coupled to the frequency scan of the gratings (linear in wavenumber units). For the experiments at room temperature, the crystals were mounted on a goniometer head that was attached to the transfer plate of the spectrometer. The plate transfers the laser beam to the crystal and the scattered light into the main lens of the spectrometer. For the low-temperature experiments, the goniometer head was mounted in a liquid ^{4}He optical cryostat which could be suspended over the transfer plate.

A Spectra-Physics krypton ion laser (model 164-01) was used with the Coderg spectrometer. It emits at a number of frequencies through the visible spectrum. The most useful radiation is the 6471-Å line which has a power in excess of 0.5 W at maximum current and lies well above the absorption edge in PbI_2.

Because of the many plasma lines which appear in the output of the laser, a diffraction grating was normally used to filter the light before it entered the transfer plate of the Coderg.[33] This caused an 80% reduction in the power of the laser beam for the 6471-Å line but the remainder was more than adequate for the experiments. The scanning speed and resolution (slit width) of the spectrometer were adjusted for optimum response.

Difficulties were sometimes encountered in determining the zero of the spectrometer (i.e., the position of the Rayleigh peak). For example, in successive scans of a spectrum, the center of the Rayleigh peak could shift by as much as 1 cm^{-1}. To determine the shift, it was therefore important to record both the Stokes and anti-Stokes components.

The output of the krypton laser was polarized in the vertical direction by the Brewster windows used in the plasma tube. The sense of polarization could be rotated by means of a double prism mounted on the front of the laser. The Coderg spectrometer contained slots for the insertion of analyzers and, by this means, both vertical and horizontal polarizations could be observed. Quarter-wave plates were also used to eliminate the grating bias to polarization direction. Since the PbI_2 crystals tended to display appreciable internal light scattering, the polarization measurements were not always as successful as was desired.

The temperature of the PbI_2 crystals was determined by the Raman effect, that is, by the ratio of the intensities of the Stokes to anti-Stokes Raman peaks. Because of the amount of blackbody radiation from the optical windows and of the heating by the laser beam, the lowest temperature obtained for the crystal was approximately 50 K.

C. Thermal-expansion measurements

A Syntex $P2_1$ diffractometer with a low-temperature attachment was used to determine the lattice parameters as a function of temperature for a small gel-grown PbI_2 crystal. The crystal was mounted on the tip of a Chromel-Alumel thermocouple attached to a goniometer head and cooled with a stream of dry-nitrogen gas that was passed through a heat exchanger immersed in a liquid-nitrogen bath. With this arrangement, it was possible to cool the crystal to temperatures as low as 100 K.

The goniometer head and the gas nozzle were mechanically coupled so that they remained aligned reasonably well as the triple-axis arrangement moved to line up various reflections. There were, however, small changes in alignment as the system was moved and they caused slight shifts in the temperature of the crystal for different reflections. The temperature variation for a given set of data was, on the average, quite small, ~3 K. It did not, therefore, have an appreciable effect on the accuracy of the lattice parameters.

The main sources of error were the small

number of reflections used (15) and the difficulty of centering the three axes of the diffractometer. If the memory of the computer attached to the diffractometer had been larger, the centering problem would have been less severe. The data were analyzed by least squares to yield hexagonal lattice parameters to ±0.003 Å for a and to ±0.016 Å for c. As will be discussed in Sec. III D, the relative values of the parameters as a function of temperature are much more precise than this.

III. RESULTS

A. Raman spectra

The observed Raman spectra of the six polytypes of PbI_2, corresponding to the temperatures 400 and 50 K, are illustrated in Figs. 2 and 3. Frequency here is in units of wave numbers (cm^{-1}). The reduction in the figures is so great that some of the detail is suppressed. The positions of peaks were read from the original recorder tracings and are listed in Table II, together with their probable uncertainties and assignments. The latter were established by arguments based on group theory, and on the knowledge of the space groups of the structures. Because of their small intensities, some active modes, which might have been expected to appear, were not observed, expecially at the lowest temperature.

A summary of published[17-21] Raman spectra of polytypes $2H$ and $4H$ of PbI_2 is given in Table III. The frequencies and the assignments correspond reasonably closely to those given in Table II.

B. Correlation with other vibrational properties

In Fig. 4, the various zone-boundary frequencies determined from the Raman spectra of the polytypes are compared with the results of inelastic neutron scattering experiments.[22] The curves drawn represent the longitudinal acoustic (LA) and doubly degenerate transverse acoustic (TA) branches of the vibration spectrum corresponding to the crystallographic c direction. They were calculated from the force-constant model to be discussed in Sec. III C. For the moment, they serve to guide the eye. The Raman frequencies for $T = 50$ K are larger than those determined at higher temperatures since the lattice contracts and stiffens at lower temperatures. As expected, no Raman features were found which correspond to the longitudinal acoustic branch observed by neutron scattering. The weak Raman peak at $\omega = 25$ cm^{-1}, noted by Nakashima,[21] remains to be explained.[18]

A more detailed analysis yields for the transverse velocity of sound in the long-wave limit:

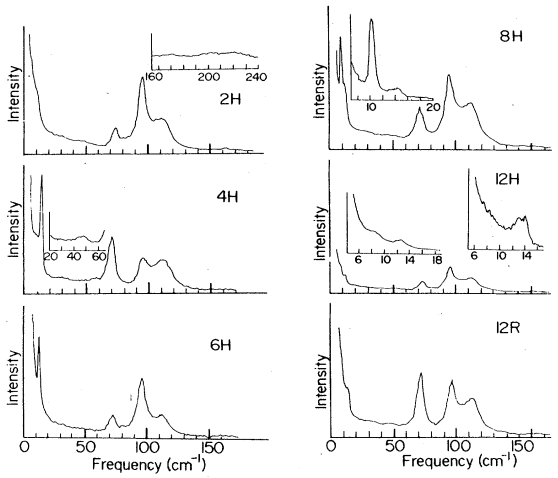

FIG. 2. Observed Raman spectra of polytypes of PbI_2 at $T = 400$ K.

$$V_t(\text{Raman}, 400\ \text{K}) = 0.87(\pm 0.06) \times 10^5\ \text{cm sec}^{-1}$$

and

$$V_t(\text{neutron}, 295\ \text{K}) = 0.93(\pm 0.02) \times 10^5\ \text{cm sec}^{-1}.$$

These nearly agree within the limits indicated with a result obtained[23] from Brillouin spectra:

$$V_t(\text{Brillouin}, 295\ \text{K}) = 1.00(\pm 0.02) \times 10^5\ \text{cm sec}^{-1}.$$

However, a comparison of *average* wave velocities from thermodynamic, inelastic neutron, and Brillouin scattering shows[34] a discrepancy between the result of the Brillouin measurements and those of the others.

A composite display of the optical branches for the c direction of the vibrational spectrum is shown in Fig. 5. More detailed comparisons for the dif-

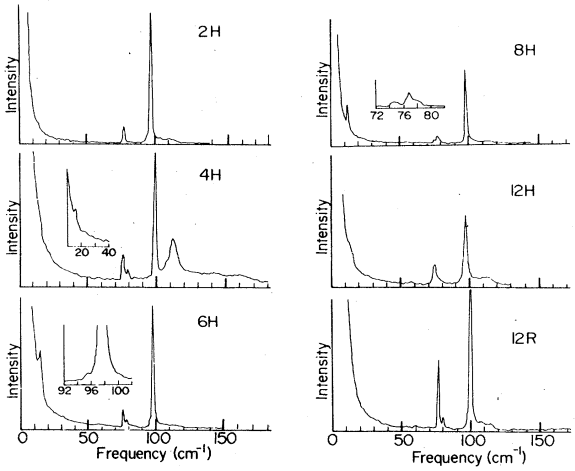

FIG. 3. Observed Raman spectra of polytypes of PbI_2 at $T = 50$ K.

TABLE II. Observed Raman spectra for PbI_2 and assignments.

Wave number (cm^{-1}) 400 K	200 K	50 K	Mode	Activity
Polytype 2*H*				
74.0 ± 0.5	76.5 ± 0.2	77.5 ± 0.5	E_g	$a_{xx}-a_{yy}, a_{xy}$ a_{yz}, a_{zx}
95.5 ± 0.5	96.8 ± 0.5	97.3 ± 0.2	A_{1g}	$a_{xx}+a_{yy}, a_{zz}$
106 ± 1	···	···	$2E_u$	T_x, T_y
113 ± 1	···	···	A_{2u}	T_z
165 ± 5	···	···	$2E_g$	$a_{xx}-a_{yy}, a_{xy}$ a_{yz}, a_{zx}
205 ± 5	···	···	$4E_u$	T_x, T_y
220 ± 5	···	···	$2A_{2u}$	T_z
Polytype 4*H*				
13.6 ± 0.2	···	15.2 ± 0.2	E_2^3	$a_{xx}-a_{yy}, a_{xy}$
48.5 ± 0.5	···	···	E_2^2, E_1^2	$a_{xx}-a_{yy}, a_{xy}$ or a_{yz}, a_{zx}, T_x, T_y
70.0 ± 0.5	74.0 ± 0.5	74.6 ± 0.2	E_2^1	$a_{xx}-a_{yy}, a_{xy}$
	···	78.1 ± 0.2	E_1^1	a_{yz}, a_{zx}, T_x, T_y
95.5 ± 0.5	96.8 ± 0.5	97.3 ± 0.2	A_1^1	$a_{xx}+a_{yy}, a_{zz}, T_z$
106 ± 1	···	···	$2E_1^2$	a_{yz}, a_{zx}, T_x, T_y
113 ± 1	···	111.1 ± 0.5	A_1^2	$a_{xx}+a_{yy}, a_{zz}, T_z$
165 ± 5	···	···	$2E_1^1, 2E_2^1$	a_{yz}, a_{zx}, T_x, T_y and $a_{xx}-a_{yy}, a_{xy}$
Polytype 6*H*				
12.8 ± 0.2	13.5 ± 0.2	13.8 ± 0.2	E^8, E^9	$a_{xx}-a_{yy}, a_{xy}$ a_{yz}, a_{zx}, T_x, T_y
72.3 ± 0.2	73.5 ± 0.5	75.5 ± 0.3	E^2, E^3	,,
···	···	77.9 ± 0.3	E^1	,,
···	···	95.1 ± 0.2	A_1^5, A_1^6	$a_{xx}+a_{yy}, a_{zz}, T_z$
95.5 ± 0.5	96.8 ± 0.5	97.3 ± 0.2	A_1^4	,,
Polytype 8*H*				
10.4 ± 0.2	11.0 ± 0.2	11.8 ± 0.2	E^{10}, E^{11}	$a_{xx}-a_{yy}, a_{xy}$ a_{yz}, a_{zx}, T_x, T_y
13.6 ± 0.5	···	15.2 ± 0.5	E^{12}	,,
···	···	74.3 ± 0.2	E^4	,,
72.4 ± 0.2	73.8 ± 0.5	76.3 ± 0.2	E^2, E^3	,,
···	···	77.9 ± 0.5	E^1	,,
95.5 ± 0.5	96.8 ± 0.5	97.3 ± 0.2	A_1^5	$a_{xx}+a_{yy}, a_{zz}, T_z$
Polytype 12*H*				
8.5 ± 0.2	···	···	E^{14}, E^{15}	$a_{xx}-a_{yy}, a_{xy}$ a_{yz}, a_{zx}, T_x, T_y
12.8 ± 0.2	···	···	E^{16}, E^{17}	,,
13.6 ± 0.2	···	···	E^{18}	,,
71.5 ± 0.2	···	75.0 ± 0.2	E^2, E^3 or E^4, E^5	,,
74.0 ± 0.5	···	78.0 ± 0.5	E^1	,,
95.5 ± 0.5	96.8 ± 0.5	97.3 ± 0.2	A_1^7	$a_{xx}+a_{yy}, a_{zz}, T_z$
Polytype 12*R*				
70.0 ± 0.5	···	74.6 ± 0.5	E_g^2	$a_{xx}-a_{yy}, a_{xy}$ a_{yz}, a_{zx}
···	···	78.1 ± 0.5	E_g^1	,,
95.5 ± 0.5	96.8 ± 0.5	97.3 ± 0.2	A_{1g}^1	$a_{xx}+a_{yy}, a_{zz}$

ferent crystal polytypes are available elsewhere.[35] The TO_2 branch is well-defined by the Raman results, as is its temperature dependence. Less information is obtained for the LO_1 and LO_2 branches but more information is available, in principle, in the infrared spectra of the 2*H* and 4*H* polytypes. Mon[49] gives the frequencies 85, 100, and 112 cm^{-1} (without experimental uncer-

TABLE III. Published Raman spectra of polytypes 2*H* and 4*H* of PbI_2.

Mode	Wave number (cm^{-1})	Temperature (K)	Reference
Polytype 2*H*			
E_g	75	295	19
	76	295	20
	74	295	18
	79.0 ± 0.5	77	17
A_{1g}	100	295	19
	94.3	295	20
	96	295	18
	98.0 ± 0.5	77	17
$2E_u, A_{2u}$	120	295	19
	101	295	20
	110	295	18
	106,113	77	17
Polytype 4*H*			
E_2^3	13.5	295	18
	15.6	9	18
	15.5 ± 0.5	77	17
E_1^2, E_2^2	51 ± 2	77	17
E_2^1	75.2	36	21
	72	295	18
	73.9	9	18
	75.0 ± 0.5	77	17
E_1^1	78.2	36	21
	77.2	9	18
	78.5 ± 0.5	77	17
A_1^1	97	36	21
	96	295	18
	98.0 ± 0.5	77	17
$2E_1^2, A_1^2$	107,112	36	21
	106,113	77	17
$2E_1^1, 2E_2^1$	151,171.8	36	21
$2A_1^2$	223.2	36	21

tainties) which can be correlated with the top three branches of Fig. 5, although it should be noted that TO_2 and LO_2 are not infrared active in 2*H* PbI_2. Another frequency given by Mon at 128 cm^{-1} is possibly an overtone of a mode at 65 cm^{-1} or a combination mode. Infrared reflectivity measurements of Grisel and Schmid[17] give an E_u (TO) mode at 52.5(±1.5) cm^{-1} and an A_{2u} (LO) mode at about 110 cm^{-1}. These agree well with the TO_1 and LO_1 curves of Fig. 5. More recent data from polarization measurements have been reported[36,37]: E_u(TO) = 52, E_u(LO) = 108, A_{2u}(TO) = 96, and A_{2u}(LO) = 121 cm^{-1}.

C. Force-constant model

To correlate the vibrational properties, we use a simple model, originally introduced by Ghosh[38] and subsequently extended and corrected by Anderson and Todoeschuck[28] to study $FeCl_2$ and $CoCl_2$. Figure 6 shows the six interlayer force constants used to describe the crystal vibrations along the *c* axis. Three constants, K_0^c, K_1^c, and

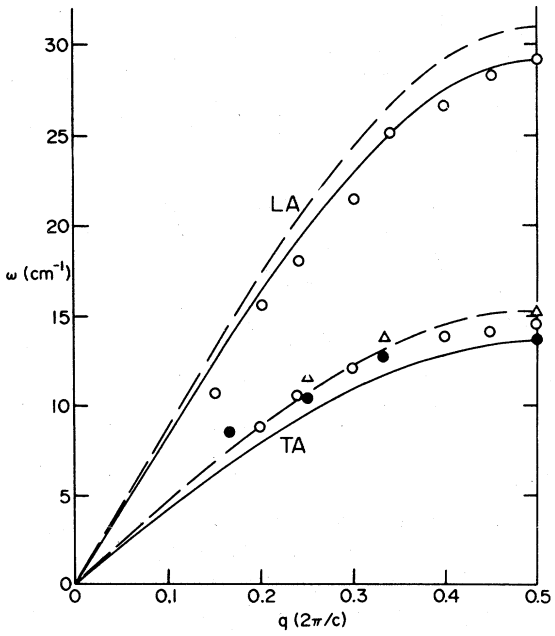

FIG. 4. Acoustic branches of dispersion curves in the *c* direction for PbI_2. ●, Raman scattering (T = 400 K); △, Raman scattering (T = 50 K); ○, inelastic neutron scattering (T = 295 K). —, (T = 400 K), --- (T = 50 K), calculated from force-constant model (Sec. III C).

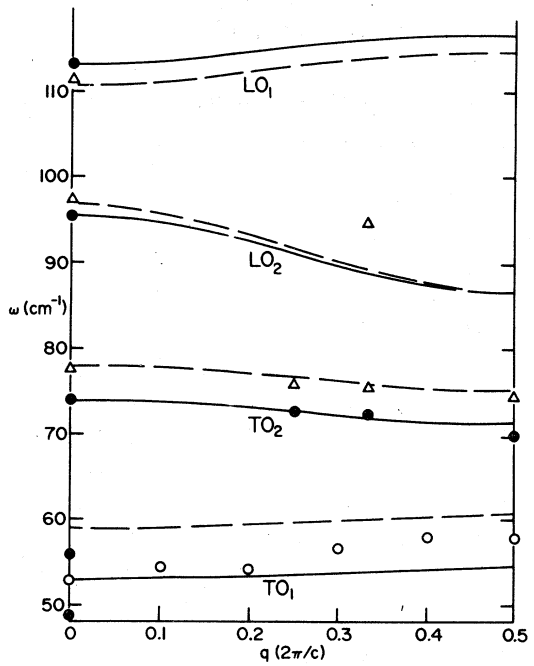

FIG. 5. Some optical branches of dispersion curves in the *c* direction for PbI_2. ●, Raman scattering (T = 400 K); △, Raman scattering (T = 50 K); ○, inelastic neutron scattering (T = 295 K); — (T = 400 K), --- (T = 50 K), calculated from force-constant model (Sec. III C).

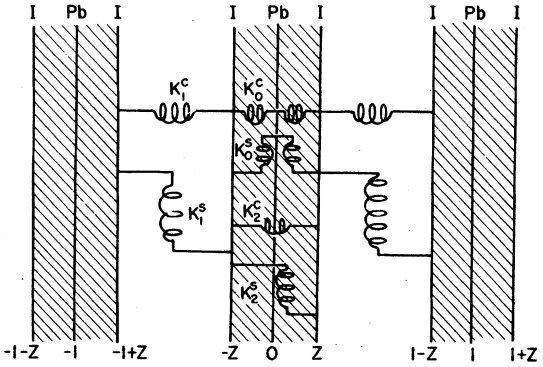

FIG. 6. Interlayer force constants for modes propagating along the c axis of PbI_2. Planes of iodide ions are located at $\pm z$ with respect to the planes of lead ions (in units of c).

K_2^c define compressional motion and K_0^s, K_1^s, and K_2^s describe shear motion. These rigid layer force constants were fitted to the zone edge and center frequencies as displayed in Figs. 4 and 5. Further details may be found in Ref. 35. Numerical values of the frequencies and of the derived force constants are given in Table IV. The eigenvectors which depict compressional modes of the $2H$ structure are shown in Fig. 7. A similar array can be identified for the doubly degenerate shear modes (E_u^2, E_g, E_u') that are perpendicular.

The dispersion curves calculated from the force constants (Table IV) yield a reasonably good fit

TABLE IV. Selected frequencies and derived force constants.

Wave number (cm^{-1})		Force constant Symbol	Value (N/m)
$T=400$ K			
	Compressional		
113 (±1)		K_0^c	43 (±1)
95.5(±0.5)		K_2^c	6.6 (±1)
29 (±2)		K_1^c	6.1 (±1)
	Shear		
53 (±3)		K_0^s	9.4 (±1)
74 (±0.5)		K_2^s	14.4 (±0.5)
13.6(±0.2)		K_1^s	1.33(±0.05)
$T=50$ K			
	Compressional		
111.1(±0.5)		K_0^c	41 (±0.5)
97.3(±0.2)		K_2^c	7.6 (±1)
31 (±3)		K_1^c	7.0 (±1)
	Shear		
59 (±3)		K_0^s	11.7 (±1)
78.1(±0.2)		K_2^s	15.3 (±0.5)
15.2(±0.2)		K_1^s	1.67(±0.05)

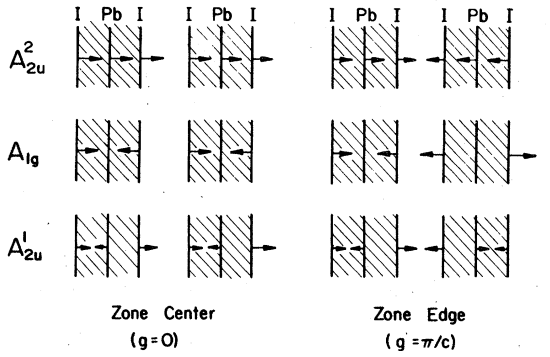

FIG. 7. Compressional rigid layer modes for polytype $2H$ of PbI_2.

(Figs. 4 and 5) to the experimental data. The dispersion predicted for the LO_1 branch by the model appears to be too large. Also, the temperature dependence of the branch seems to be different from that of the other branches. One experimental point on the TA branch, derived from the spectrum of $12H$ polytype, deviates more than the others but, as is evident from Fig. 2, the spectral feature from which it is derived is not well defined.

In Table IV, we see that the weakest force constant (K_1^s) corresponds to the shearing of the PbI_2 layers. The strongest shear constant (K_2^s) corresponds to the iodine-iodine interaction across the layer. As would be expected, the inter-PbI_2 compressional force constant is by far the strongest.

D. Thermal expansion

The measured a- and c-lattice parameters as a function of temperature are given in Table V. For room temperature, Wyckoff[39] gives $a=4.557$ and and $c=6.979$ Å and these agree well with $a=4.5562(\pm0.0004)$ and $c=6.9830(\pm0.0004)$ Å obtained by Sirdeshmukh and Deshpande.[40] Because of the diffractometer centering difficulties mentioned in Sec. II C, the data in Table V probably contain small systematic errors. In order to correlate

TABLE V. Lattice parameters of PbI_2 ($2H$).

T (K)	a (Å)	c (Å)
102	4.524(±0.003)	6.899(±0.016)
121	4.525	6.908
140	4.526	6.914
162	4.527	6.913
187	4.531	6.923
215	4.534	6.930
244	4.538	6.937
276	4.543	6.944
293	4.547	6.946

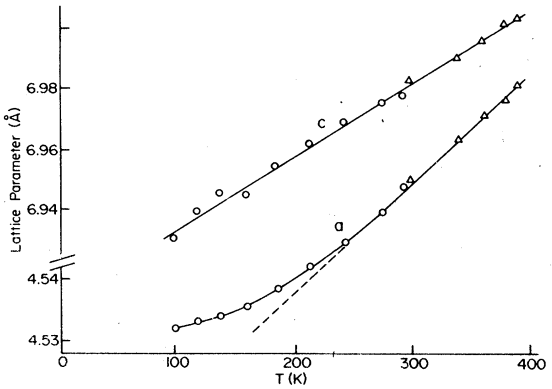

FIG. 8. Lattice parameters of PbI_2 as a function of temperature O, present measurements (shifted); Δ, Ref. 40.

the thermal-expansion data, the results for a and c were shifted by 0.008 and 0.032 Å, respectively. The consequences are displayed in Fig. 8. It is clear that the temperature dependences of the two sets of measurements correspond very well.

The contraction of the PbI_2 layers in the c direction is linear in T down to the lowest experimental temperature; $dc/dT = 2.5(\pm 0.1) \times 10^{-4}$ Å/K. Along the a direction, on the other hand, the expansivity decreases for $T < 250$ K in accordance with the premise that intralayer forces are stronger than interlayer (c direction) forces and hence "freeze out" sooner. In the region of room temperature, $da/dT = 1.80(\pm 0.05) \times 10^{-4}$ Å/K and $\alpha_\perp = (1/a)(da/dT) = 4.0(\pm 0.1) \times 10^{-5}$ K^{-1}. In addition, $\alpha_\parallel = (1/c)(dc/dT) = 3.6(\pm 0.1) \times 10^{-5}$ K^{-1} and so the volume expansivity at room temperature becomes $\alpha = 1.16(\pm 0.03) \times 10^{-4}$ K^{-1}. This result is to be compared with $\alpha = 1.008 \times 10^{-4}$ K^{-1} and $\alpha = 1.086 \times 10^{-4}$ K^{-1} reported by Fizeau[41] and by Klemm *et al.*,[42] respectively.

For axial crystals, it is convenient to define two Grüneisen parameters[43-45]

$$\gamma_a = (V/C_\sigma)[(c_{11} + c_{12})\alpha_a + c_{13}\alpha_c] \quad (1)$$

and

$$\gamma_c = (V/C_\sigma)(2c_{13}\alpha_a + c_{33}\alpha_c), \quad (2)$$

where V is the volume, C_σ is the heat capacity at constant stress, and c_{ij} are the elastic constants. To obtain estimates of γ_a and γ_c at room temperature, we take $C_\sigma = 80$ J/mole K (essentially the classical value of C_p) and elastic constants from measurements of Brillouin spectra.[23] We obtain $\gamma_a = 1.8$ and $\gamma_c = 1.6$.

To the extent that PbI_2 has a layer-type structure, the thermal expansion parallel to the c axis can be calculated by an anharmonic-linear-chain model. Thus, if f_0 is the harmonic interlayer force constant corresponding to the interlayer spacing c_0, we can write

$$f(c) = f_0 + g_0(c - c_0) + \cdots, \quad (3)$$

where g_0 is the cubic anharmonic force constant that gives rise to thermal expansion. From a detailed microscopic model,[46] the Grüneisen parameter for this one-dimensional solid is

$$\gamma = -c_0 g_0 / 2f_0. \quad (4)$$

Moreover, we can also derive

$$\Delta c = c - c_0 = -(g_0/2f_0^2)(k_B T) \quad (5)$$

and hence

$$\frac{dc}{dT} = -\frac{g_0}{2f_0^2} k_B. \quad (6)$$

From the experimental value of dc/dT, we obtain $g_0/2f_0^2$. If we assume that the predominant expansion occurs between layers of PbI_2, we can identify f_0 with K_1^c and c_0 with the interlayer separation (cf. Fig. 6): $(1 - 2Z)c = 0.47c$ (Ref. 5). In this way, we find $\gamma = 3.6$ which is about twice as large as γ_c given above. This shows that it is an oversimplification to attribute all of the anharmonicity to the variation of K_1^c with temperature and that the layer-like character of PbI_2 cannot be extreme. It is possible that a more consistent picture of the thermal expansion could be developed from an atom-atom model of the type used by Maiti and Ghosh.[27]

IV. SUMMARY

The simple force-constant model used to correlate the vibrational properties of PbI_2 works surprisingly well. In particular, it yields a good description of dispersion of the lattice waves in the c direction. It even accounts for a large part of the anharmonicity in the vibrations. The force constants, derived from the model, lead to the conclusion that PbI_2 displays much less two-dimensional character than graphite or MoS_2. This is illustrated in Table VI. The ratio K_1^s/K_0^c and K_1^c/K_0^c measure the relative significance of interlayer to intralayer forces.

The next stage of refinement for calculations should be the detailed development of microscopic models. These would be facilitated if additional experiments were performed, especially measurements of Brillouin and infrared spectra and inelastic neutron scattering down to low temperatures.

ACKNOWLEDGMENTS

The authors would like to thank J. D. Garrett and Dr. J. E. Greedan for assistance with the cry-

TABLE VI. Comparison of force-constant ratios for selected layer type crystals.

Crystal	K_1^s/K_0^s	K_1^c/K_0^c	Reference
Graphite	0.001	0.010	47
MoS_2	0.014	0.038	47
$CoCl_2$	0.021(±0.002)	0.112(±0.007)	28
$FeCl_2$	0.025(±0.002)	0.090(±0.005)	28
PbI_2	0.035		18
	0.031(±0.002)	0.14(±0.03)	Present results

stal growing, Dr. H. E. Howard-Lock for the loan of the Raman spectrometer, R. Faggiani for assistance with the x-ray measurements and, especially, Dr. A. Pasternak for helpful discussions and correspondence. The financial support of the National Research Council of Canada is gratefully acknowledged.

*Present address: Dept. of Physics, University of Guelph, Guelph, Ontario, Canada.

[1]A. R. Verma and P. Krishna, *Polymorphism and Polytypism in Crystals* (Wiley, New York, 1966).
[2]L. S. Ramsdell, Am. Mineralogist 32, 64 (1947).
[3]J. I. Hanoka, K. Vedam, and H. K. Henisch; *Proceedings of an International Conference on Crystal Growth, Boston, June 20–24,* 1966, edited by H. S. Peiser (Pergamon, London, 1967), p. 369.
[4]R. Prasad, J. Phys. Chem. Solids 37, 337 (1976).
[5]R. S. Mitchell, Z. Kristallogr. 111, 372 (1959).
[6]W. J. Choyke and L. Patrick, Phys. Rev. 172, 769 (1968).
[7]L. Patrick, Phys. Rev. 167, 809 (1968).
[8]D. W. Feldman, J. H. Parker, Jr., W. J. Choyke, and L. Patrick, Phys. Rev. 170, 698 (1968).
[9]C. H. Hodges, Phys. Rev. 187, 994 (1969).
[10]M. R. Tubbs, Phys. Status Solidi B 49, 11 (1972).
[11]T. Yao and I. Imai, Solid State Commun. 9, 205 (1971).
[12]A. E. Dugan and H. K. Henisch, J. Phys. Chem. Solids 28, 971 (1967).
[13]F. Levy, A. Mercier, and J. P. Voitchovsky, Solid State Commun. 15, 819 (1974).
[14]A. E. Dugan and H. K. Henisch, Phys. Rev. 171, 1047 (1968).
[15]M. Yashiro, T. Goto, and Y. Nishina, Solid State Commun. 17, 765 (1975).
[16]L. C. Thanh, C. Depeursinge, F. Levy, and E. Mooser, J. Phys. Chem. Solids 36, 699 (1975).
[17]A. Grisel and Ph. Schmid, Phys. Status Solidi B 73, 587 (1976).
[18]R. Zallen and M. L. Slade, Solid State Commun. 17, 1561 (1975).
[19]J. P. Mon, C. R. Acad. Sci. Paris Ser. B 262, 493 (1966).
[20]C. Carabatos, C. R. Acad. Sci. Paris Ser. B 272, 465 (1971).
[21]S. Nakashima, Solid State Commun. 16, 1059 (1975).
[22]B. Dorner, R. E. Ghosh, and G. Harbeke, Phys. Status Solidi B 73, 655 (1976).
[23]J. Sandercock, Festkörperprobleme XV, 183 (1975).
[24]A. Pasternak, J. Phys. C 9, 2987 (1976).
[25]See R. Zeyher, *Lattice Dynamics*, edited by M. Balkanski (Flammarion, Paris, 1977), p. 17 for details of unpublished work by A. Frey.
[26]N. S. Gillis, Phys. Rev. B 3, 1482 (1971).
[27]C. R. Maiti and P. N. Ghosh, J. Phys. C 11, 2475 (1978).
[28]A. Anderson and J. P. Todoeschuck, Can. J. Spectrosc. 22, 113 (1977).
[29]H. K. Henisch, *Crystal Growth in Gels* (Pennsylvania State University, University Park, 1970).
[30]H. K. Henisch, J. Dennis, and J. I. Hanoka, J. Phys. Chem. Solids 26, 493 (1965).
[31]R. Prasad and O. N. Srivastava, J. Cryst. Growth 19, 11 (1973).
[32]T. Nimagawa, Acta Crystallogr. A 31, 823 (1975).
[33]K. Jain, W. T. Wozniak, and M. V. Klein, Appl. Opt. 14, 811 (1975).
[34]W. M. Sears and J. A. Morrison, J. Phys. Chem. Solids (to be published).
[35]W. M. Sears, Ph.D. thesis (McMaster University, Hamilton, Ontario, 1978).
[36]G. Lucovsky, R. M. White, W. Y. Liang, R. Zallen, and Ph. Schmid, Solid State Commun. 18, 811 (1976).
[37]G. Lucovsky and R. M. White, Nuovo Cimento B 38, 290 (1977).
[38]P. N. Ghosh, Solid State Commun. 16, 811 (1975).
[39]R. W. G. Wyckoff, *Crystal Structures*, 2nd ed., Vol. 1 (Interscience, New York, 1963).
[40]D. B. Sirdeshmukh and V. T. Deshpande, Current Sci. 41, 210 (1972).
[41]H. Fizeau, C. R. Acad. Sci. Paris 64, 771 (1867).
[42]W. Klemm, W. Tilk, and S. V. Müllenheim, Z. Anorg. Allg. Chem. 176, 1 (1928).
[43]R. W. Munn, Adv. Phys. 18, 515 (1969).
[44]R. W. Munn, Philos. Mag. 17, 433 (1968).
[45]T. H. K. Barron and R. W. Munn, Philos. Mag. 15, 85 (1967).
[46]M. Born and K. Huang, *Dynamical Theory of Crystal Lattices* (Oxford, Oxford, England, 1954), p. 60.
[47]R. Zallen and M. Slade, Phys. Rev. B 9, 1627 (1974).

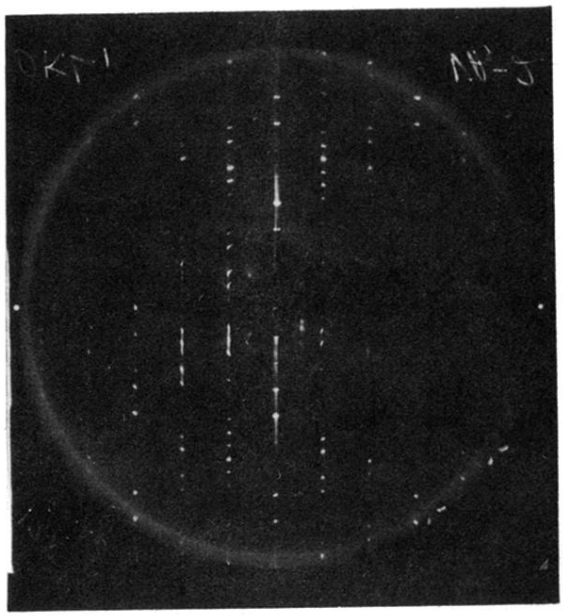

FIG. 1. X-ray photograph of polytype $12R$ (reverse) of PbI_2 in the O, K, L reciprocal plane.